MAGNETIC RESONANCE IN MEDICINE 21, 197–215 (1991)

Human Auditory System Response to Pulsed Radiofrequency Energy in RF Coils for Magnetic Resonance at 2.4 to 170 MHz

PETER RÖSCHMANN

Philips GmbH Forschungslaboratorium Hamburg, D-2000 Hamburg 54, Vogt-Kölln-Str. 30, Federal Republic of Germany

Received June 20, 1990; revised Spetember 24, 1990

The threshold conditions for an auditory perception of pulsed radiofrequency (RF) energy absorption in the human head have been studied on six volunteers with RF coils for magnetic resonance (MR) imaging. For homogeneous RF exposure with MR head coils in the 2.4- to 170-MHz range and pulse widths 3 $\mu s \leq T_p < 100$ μs, the auditory thresholds were observed at 16 ± 4 mJ pulse energy. Localized RF exposure with optimized surface coils positioned flush with the ear lowers the auditory threshold to only 3 ± 0.6 mJ. The hearing threshold of RF pulses with $T_p > 200$ μs occurs at more or less constant peak power levels of typically 150 ± 50 W for head coils and as low as 20 W for surface coils. The results from this study confirm theoretical predictions from a thermoeleastic expansion model and compare well with reported thresholds from near field antenna measurements at 425 to 3000 MHz. Details of the threshold dependence on RF pulse length reveal primary sites of RF to acoustic energy conversion at the mastoid and temporal bone region and the outer layer of the brain from where thermoelastically generated pressure transients excite audible pressure waves at the resonance modes of the skull around 1.7 kHz and of the brain around 11 kHz. If not masked by usually dominating noise from switched gradients, the conditions for hearing RF pulses, as applied to head coils in MR studies with flip angle α at main field B_0, is given by $T_p/\text{ms} \leq 0.4\,(\alpha/\pi)B_0/[T]$. At peak power levels up to 15 kW presently available in clinical MR systems, there is no evidence known for detrimental health effects arising from the RF auditory phenomenon which is a secondary cause associated with primary RF to thermal energy conversion in body tissues. To avoid the RF-evoked sound pressure levels in the head rising above the discomfort threshold at 110 dB SPL, an upper limit of 30 kW applied peak pulse power is suggested for head coils and 6 kW for surface coils.

INTRODUCTION

When pulsed RF energy of appropriate level is absorbed in the human head, an audible sound is generated which can be perceived as a click or chirp originating from a region within or behind the back of the head. The RF auditory phenomenon has been reported for frequencies of 425 up to 3000 MHz with audibility thresholds occurring at peak power densities of 0.1 to 40 W/cm^2 for pulse widths between 1 ms and 1 μs, respectively (*1–4*). A theoretical analysis of various physical transduction mechanisms has shown that thermoelastic expansion is about three orders of magnitude more effective than other possible mechanisms like electrostriction or radiation pressure in converting RF energy into acoustic energy (*5, 6*). The absorption of pulsed RF

0740-3194/91 $3.00

energy in the brain causes a miniscule ($\sim 10^{-5}$ °C) but rapid (~ 10 μs) rise of temperature. The resultant thermoelastic expansion launches acoustic waves of pressure at the vibrational eigenfrequency of the human brain near 12 kHz. Via bone conduction the RF-evoked short bursts of sound waves arrive at the cochlea and are detected by the hair cells.

The peak power levels and the duration of RF pulses used for MR imaging and spectroscopy of the human head can be well compatible with the requirements for evoking an auditory response by electromagnetic energy. This applies in particular to MR spectroscopy and Na imaging at higher values of the main field in the 1–4 T range. The perception of RF-evoked auditory sound within a MR head coil was noted for the first time by the author when volunteering in a ^{1}H spectroscopic imaging experiment performed with a 4-T whole-body MR system. In the course of one of the experiments the gradient power supply broke down, while the RF pulse sequence continued to run. Without the masking acoustic noise from the switched gradients being present, the used three $\pi/2$-RF pulses (6 kHz sinc pulses with 3 kW peak power level) of a spectroscopic imaging sequence could be heard clearly as three distinct clicks in the rhythm of the interpulse delays of 150 and 50 ms with repetition time of 1.5 s. The use of different MR head or surface coils in the 2- to 170-MHz range for investigations of the RF auditory effect offers a complementary as well as an alternative experimental approach to previously reported studies at higher frequencies (*1–4*). In these studies the subjects were exposed to the electromagnetic RF field within the Fresnel region (near zone) of horn antennas, where uncertainties arise in determining the effective RF power density in the presence of an inhomogeneous object such as the human head with permittivity in the order of $\epsilon_r \approx 50$. Apart from the different frequency range explored, the use of RF coils also provides a different mode of RF power deposition which is predominantly of an inductive nature via the interaction of the coil's RF magnetic field with electrically conductive tissues of the head. Moreover, RF coils enable exact measurements of the amount of RF power absorbed in the human head.

A brief account on initial measurements of RF auditory threshold power levels observed with MR head coils for 8 to 170 MHz was given previously (*7*). This paper presents results from an extended range of the RF auditory threshold parameters of radiofrequency, pulse duration, pulse repetition rate, and peak power level for exposures to both localized and homogeneous RF magnetic fields. These threshold results provide clues to further understanding of the primary sites of interactions and of the share of different acoustic head resonance modes. Conditions for RF hearing during MR imaging or spectroscopy studies, possible annoyance levels, and health risk questions are delineated.

METHODS AND EXPERIMENTAL PROCEDURES

Measurements of RF audibility threshold parameters were performed using the RF transmitter signal path of the spectrometer equipment of an experimental 4-T whole-body broadband MR system (*8*), and different MR head and surface coils with resonance frequencies in the range from 2.4 to 170 MHz. The timing parameters in the RF pulse sequences used were software controlled. The standard RF pulse sequence

for studies of the effects of RF pulse length consisted of three equidistant rectangular pulses with an interpulse delay of T_r = 150 ms. The common pulse length T_p was varied between 3 μs $\leq T_p \leq$ 5000 μs. The sequence repetition time was TR = 1.2 s; in some cases the TR had to be increased to 3 s in order to keep the average local RF power deposition below the recommended safety limit of 5 W/kg. Effects of the pulse presentation rate on the behavioral threshold were investigated with pulse trains of T_p = 100 μs pulses at interpulse rates varied between 1 Hz $\leq 1/T_r <$ 5000 Hz. For $1/T_r \geq$ 3.3 Hz the pulse trains had a constant duration of 300 ms, and the repetition time of the pulse train sequence was TR = 1.2 s.

Six volunteers from the MR research group in our laboratory participated in this study. The positions of the RF coils around the volunteer's head are depicted in Fig. 1 along with the attained directions of the RF magnetic field (B_1). The head coils providing a transverse B_1 were saddle coils and transverse electromagnetic field (TEM) transmission line resonators. A change from the mostly applied anterior–posterior B_1 orientation to lateral B_1 was accomplished by 90° rotation of the head coil. A 2.4-MHz loop array head coil (*9*) with axial B_1 provides the caudal–cranial B_1 orientation. Circular surface coils, with RF power deposition essentially localized within a depth of less than the coil radius, were used to explore the regional efficiency dependence of RF to acoustic energy conversion on the surface of the head. During the initial phase of the study, some of the RF audition experiments were made immediately following test sessions of MR imaging or spectroscopy sequences performed with volunteers for head positions at the isocenter of the 4-T whole-body magnet. The main part of the experiments, however, was performed outside the 4-T magnet where the stray field level was below 100 G at the volunteer's head.

A plastic foam ear muff was used to attenuate acoustic noise from the environment. The volunteer was isolated from the experimenter. The RF equipment and operator console for MR system control are located in separate rooms outside the magnet

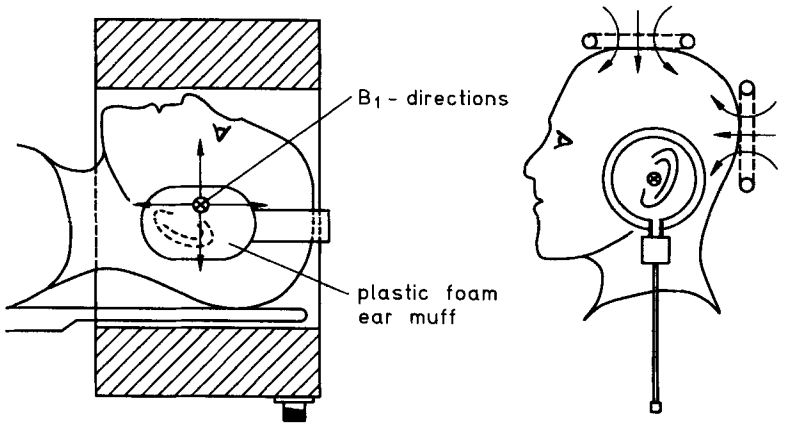

FIG. 1. Experimental arrangement of MR head and surface coils for threshold measurements of auditory sensations evoked by pulsed RF energy absorption in the human head.

room. A bell served for communication between volunteer and experimenter during the psychophysical experiments for determination of RF audibility thresholds. The following simple signal scheme proved to be reliable in obtaining reproducible threshold results within reasonable experiment time after one or two training runs were made at the beginning of a measurement series. A short double ringing of the bell informed the volunteer that a RF pulse sequence was started at a RF power level well below the audibility threshold value. The applied RF peak power level P_i at the coil input was then increased in 1-dB steps at about 10-s intervals. When the volunteer perceived the onset of an auditory sensation, he signaled the experimenter with a double ringing of the bell. After accommodation for about 30 s at the onset threshold level $P_{thr}(+)$ for initial perception, a single bell ringing informed the volunteer that P_i was now to be decreased in 1-dB steps at 10-s intervals until the volunteer signaled the disappearance of the RF auditory sensation. The RF pulse sequence was stopped after a confirming period of about 30 s at the disappearance level $P_{thr}(-)$. It has been found that $P_{thr}(+)$, $(-)$ usually differed by 1 dB, rarely by 2 dB. The average of both values is defined as the RF audibility threshold peak power level P_{thr}.

The incident (P_i) and reflected (P_r) peak power levels at the RF coil input were measured with calibrated bidirectional couplers, taking into account the frequency-dependent loss of the 20-m coaxial cable between the 5-kW broadband RF amplifier and the RF coil input. From quality factors measured for the empty RF coil (Q_{oe}), and after loading the coil with the head (Q_{oh}), the amount of RF power absorbed in the head (P_a) is obtained from

$$P_a = (P_i - P_r)\left(1 - \frac{Q_{oh}}{Q_{oe}}\right). \qquad [1]$$

The transient response of the resonant RF coil to short RF pulses (*10*) has been considered in cases where the ratio of RF pulse length T_p to the transient time constant, $\tau = Q_{oh}/\omega$, of the matched RF coil (loaded with the head) falls below a value of 20:1, see Table 1.

RF AUDITORY THRESHOLD RESULTS

Measurements with MR Head Coils

Threshold peak power levels measured for a volunteer as a function of RF pulse length with a proton head coil for 4 T (170.4 MHz) are shown in Fig. 2. The threshold results obtained with head position at the isocenter of the 4-T magnet are almost identical to those measured outside the magnet. The onset and disappearance levels $P_{thr}(+)$, $(-)$ differ primarily just by the used 1-dB decrement of the input power variation. Thus, a surprisingly well-defined threshold response is obtained from these psychophysical RF audition experiments. For pulse lengths above 60 μs, the threshold depends strongly on the orientation of the applied RF magnetic field with respect to the head. The oscillatory course of $P_{thr}(T_p)$ indicates the presence of acoustic interference, which may reduce the efficiency of RF to acoustic energy conversion at certain RF pulse lengths. An enormous difference in conversion efficiency is inferred from the threshold results in Fig. 2 for the two applied B_1 orientations when $T_p > 200$ μs.

TABLE 1

Performance Parameters of MR Coils Used for Studies of the RF Auditory Effect and RF Auditory Threshold Energies for the Investigated MR Coil–Volunteer Combinations

	Frequency $\omega/2\pi$ (MHz)	Loaded/ empty Q Q_{oh}/Q_{oe}	Transient time const. $\tau = Q_{oh}/\omega$ (μs)	W_{thr} (mJ) at $T_p \leq 50$ μs for volunteer X (age in years)					
				C (30)	T (32)	D (33)	G (39)	J (34)	P (53)
Head TEM lateral B_1	170.4	45/1092	0.04	—	—	—	—	~20	—
Head ant.–post. B_1	170.4	55/1092	0.05	—	—	—	(18)	20, 20 (16)	(18) (24)
Head TEM quadrature	170.4	54/1487	0.05	—	—	14	—	—	(20)
Head saddle	86	55/907	0.10	12	—	—	—	—	—
Head saddle	45	149/838	0.53	(18)	—	—	(20)	—	16
Head saddle	8	286/727	5.7	—	—	—	—	—	13
Head loop array	2.4	510/1090	34	—	~13	—	—	—	—
Surface coil 12 cm	43	52/794	0.19	—	—	—	—	15	—
10 cm	170	66/773	0.06	—	—	12	—	—	(16)
7 cm	85	66/451	0.12	—	(2.4)	—	—	3.6 (3)	(4.5)
7 cm	69	79/436	0.18	—	—	—	—	7	—
5.5 cm	69	78/645	0.18	—	—	—	—	9	—

Note. Underlined entries of W_{thr} were measured at 4 T; bracketed (entries) of W_{thr} are taken from control measurements not included in Figs. 2–6.

This points to several interrelated effects being involved. Localized RF power deposition occurs at different regions of the head when the direction of the applied homogeneous B_1 field is changed. RF to acoustic energy conversion by thermoelastic generation of acoustic pressure waves takes place at different preferential regions, from which, if excited by RF, acoustic waves are launched at different audio frequency ranges. For short pulse lengths, $T_p < 30$ μs, the thresholds shown in Fig. 2 for different B_1 orientations almost converge. Here, a constant pulse energy deposition of $W_{thr} = P_{thr}T_p \approx 20$ mJ was required to elicit RF-induced auditory response for the volunteer (J) with the specific head coil used.

The RF auditory thresholds shown in Fig. 3 were measured with different head coils at frequencies between 2.4 and 170.4 MHz for axial (2.4 MHz) or anterior–posterior B_1 orientation. Since the availability not only of the volunteers but also of free time gaps for the 4-T system use was limited, a random participation of the six volunteers had to be accepted in performing the RF auditory experiments. Nevertheless, a remarkable agreement within 2 to 3 dB exists for the behavioral thresholds in Fig. 3 representing data obtained for the randomly arising combinations among five volunteers and the six different RF head coils used operating at frequencies over a range of more than six octaves. Noteworthy is also the excellent agreement with literature data (*3*) from horn antenna measurements at 2450 MHz, which have been included

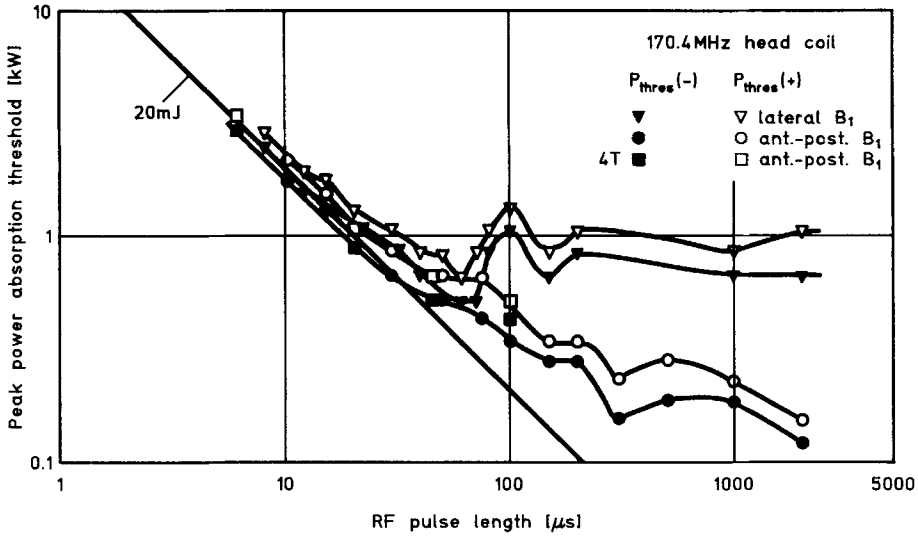

FIG. 2. RF peak power thresholds for onset (+) and disappearance (−) of the RF auditory effect versus the RF pulse length for different orientations of the applied RF magnetic B_1 field. The thresholds observed with the volunteer's head at the isocenter of the 4-T magnet are practically identical to those measured outside the magnet. A standard pulse sequence of three pulses with 150-ms interpulse delay and TR = 1.2 s was used.

in Fig. 3, using for conversion of reported peak power density data into absorbed peak power levels the reasonable assumption of an effective head absorption area of 400 cm^2.

The randomly arising combinations among the six volunteers and the 11 different RF coils used in this investigation are listed in Table 1 together with the (short) pulse energy thresholds obtained for these combinations. None of the participating volunteers was aware of any kind of subjective hearing loss, which is evidently confirmed by the uniformity of the (head coil) thresholds in Table 1 with deviations of just ±1 dB.

The dependance of the RF threshold on RF pulse length in Fig. 3 gradually changes in the transition range, 30 $\mu s < T_p < 300$ μs, from constant pulse energy threshold to constant peak power threshold as a function of T_p. The extrapolations of the $W_{thr}(T_p)$ = const. (= $W_{thr}(\min)$) and the $P_{thr}(T_p)$ = const. (= $P_{thr}(\min)$) characteristics intersect at the common value of $T_p \approx 120$ μs for all cases in Fig. 3 presenting data for $T_p > 100$ μs. Moreover, beyond the first minimum of P_{thr}, which is observed at the common value of $T_p \approx 300$ μs, there is a secondary maximum of P_{thr} about 2 to 3 dB above $P_{thr}(\min)$ at the common value of $T_p \approx 600$ μs. These common dependencies of T_p will be further discussed below along with similar results found with surface coils.

Measurements with MR Surface Coils

RF auditory thresholds obtained with a 10-cm circular surface coil at 170 MHz at different locations on the volunteer's head (see Fig. 1) are presented in Fig. 4. Several

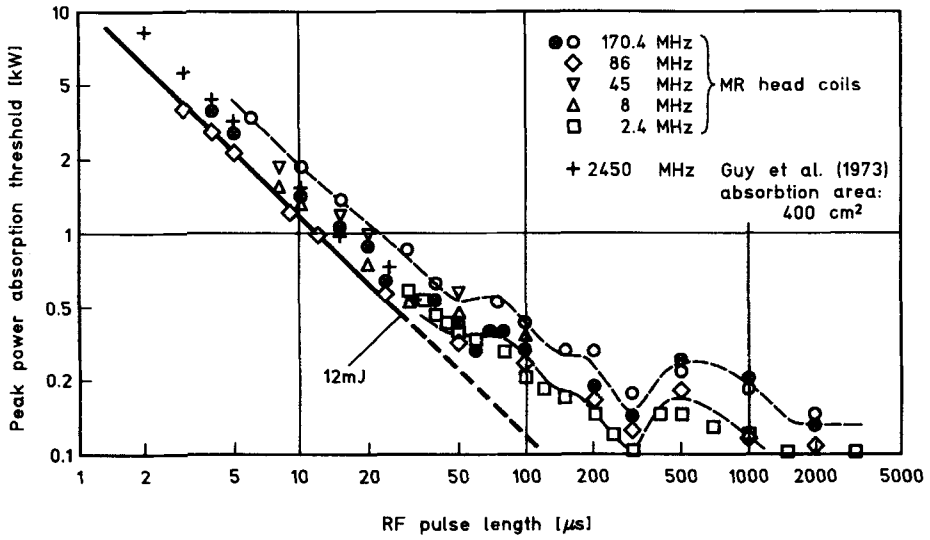

FIG. 3. RF auditory thresholds for the standard pulse sequence versus the RF pulse length for different MR head coils mostly with anterior–posterior B_1 orientation (±45 degrees off this direction for the two orthogonal systems of the 170.4 MHz quadrature coil is represented by open circles with inserted cross; the 2.4-MHz coil provides a caudal–cranial orientation of B_1). Excellent agreement is found with peak power density thresholds reported in the literature for near field antenna measurements at 2450 MHz when assuming an effective head absorption area of 400 cm^2. Data for the 45-, 8-, and 2.4-MHz coils have been corrected for the effect of transient response to short RF pulses in cases where $T_p \leq 20\ \tau$ (transient time constant of the head-loaded coil, $\tau = Q_{oh}/\omega$, see Table 1).

features of the threshold versus pulse length dependence are similar to the threshold results for different B_1 orientations of a head coil shown in Fig. 2, namely:

—a converging value of the pulse-energy threshold toward short pulse lengths, $T_p < 30\ \mu s$, for different B_1 orientations,
—a large difference in the efficiency of RF to acoustic energy conversion for different B_1 orientations when $T_p > 200\ \mu s$,
—the thresholds for the surface coil positioned at the back of the head are, except for the missing (smeared out) minimum at $T_p = 300\ \mu s$, nearly identical to the thresholds for the 2.4 or 86-MHz head coils shown in Fig. 3,
—the same positions of the first minimum of P_{thr} at $T_p \approx 300\ \mu s$ and of the secondary maximum at $T_p \approx 600\ \mu s$ are found for the respective optimum orientations of B_1 with the highest efficiency in RF to acoustic energy conversion (see also Fig. 5).

More details of auditory threshold features observed for localized RF exposure with surface coils of different diameters are shown in Fig. 5. The surface coils were positioned flush with the ear where the conversion efficiency was found to be optimum. Several notable differences are found when comparing the threshold results for homogeneous B_1 field exposure by head coils in Figs. 2 and 3 with those for localized B_1 field exposure by surface coils in Figs. 4 and 5, namely:

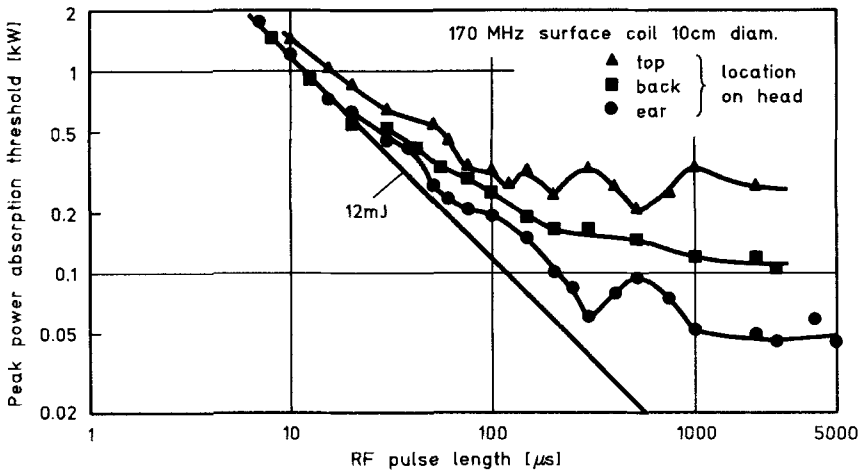

FIG. 4. RF auditory thresholds versus the RF pulse length for a MR surface coil located at different regions of the head. The standard pulse sequence was used.

—the B_1 directions for highest and lowest conversion efficiency with head coils are exactly opposite to those for surface coils,
—up to five times lower thresholds are found with surface coils,
—the constant energy–constant power threshold characteristics intersect at a common value of $T_p \approx 120$ μs for head coils and at $T_p \approx 200$ μs for surface coils.

From Fig. 5 it is seen that the increasingly localized RF power deposition obtained with surface coils of smaller size not only reduces the threshold levels but also changes the characteristic of the transition from W_{thr} = const. to P_{thr} = const. as a function of T_p. Apparently, the range of transition as well as the deviations of threshold data from the linear (ideal) dependence on T_p correlate with the RF–acoustic conversion efficiency. The smallest effects are found for the case of highest conversion efficiency as observed with the 7-cm-diameter coil at 85 MHz. However, conclusions regarding the optimum coil diameter for highest RF–acoustic conversion efficiency cannot be made yet from the few cases studied so far. The observed 3-dB difference in the thresholds of the two coils of same diameter (7 cm) operated at 69 and 85 MHz arises presumably from missing the optimum of coil location on the head, which becomes most critical for coils having close to optimum conversion efficiency.

The perception of RF-evoked sound was described by the volunteers with the following more or less unanimous subjective observations. The applied standard RF pulse sequence with short RF pulses of $T_p < 50$ μs was perceived as three distinct chirps or clicks of high pitch, originating from a region within or behind the back of the head when using head coils; when using surface coils the source of sound appeared to be located at regions of the head close to the coil. For longer RF pulses with $T_p > 100$ μs, the perceived RF evoked sound events changed to creaky or gnashing clacks of lower pitch with a somewhat longer duration. The total head appeared to be involved

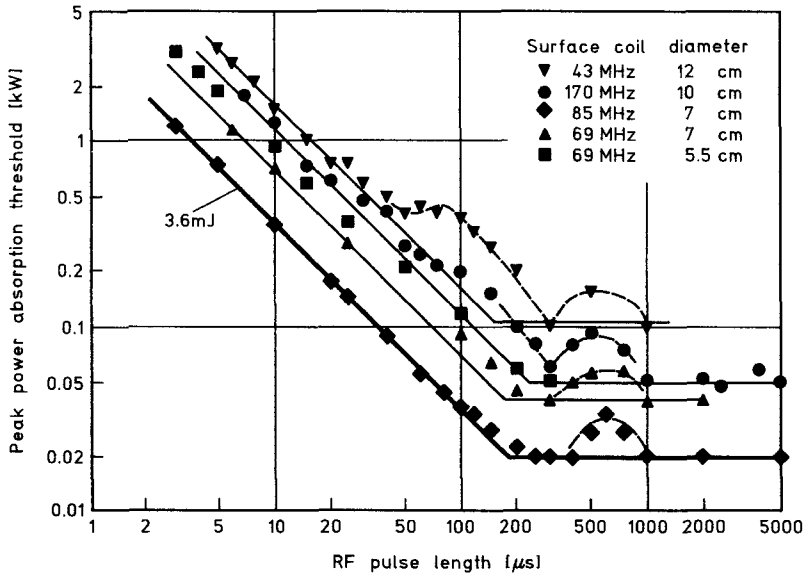

FIG. 5. RF auditory thresholds versus the RF pulse length for different MR surface coils positioned flush with the ear and applied standard pulse sequence.

as sound source when using head coils; for surface coils the sound originated from a head region close to the coil.

The RF auditory thresholds presented thus far were measured with the pulse length as the variable in a standard RF pulse sequence of three equidistant (150 ms) pulses, which corresponds to a pulse presentation rate of 6.7 Hz with 300 ms duration. The hearing threshold of the auditory system is known to depend strongly on the audio frequency. Similar behavioral effects on the RF auditory threshold were observed when using the RF pulse presentation rate as the variable in the threshold measurements. Figure 6 presents the reduction of the RF auditory threshold level measured as a function of the pulse presentation rate for two different surface coils positioned flush with the left ear of the same volunteer (J). The threshold level for a single pulse (T_p = 100 μs) sequence with a 1-Hz repetition rate was used as reference value. The RF pulse trains with pulse rates varied between 3.3 and 4975 Hz (300 ms and 201 μs interpulse delay, respectively) were applied in time slots of 300 ms duration and a repetition time of TR = 1.2 s in accordance with the standard pulse sequence. For pulse rates above 2500 Hz, an increase to Tr = 3 s was required in order to keep the average power deposition level below 1 *W*. For comparison, Fig. 6 also shows the rate-dependent reduction of the sound pressure threshold for external acoustic stimuli as measured for 100-μs earphone clicks (*11*) and for pure tones supplied monaurally by earphones (*12*). Curve fitting to the RF threshold results was performed at the lowest rate of 5 clicks/s reported for earphone clicks, which determined the absolute scale of sound pressure level (SPL) relative to $2 \cdot 10^{-5}$ N/m^2 shown on the right

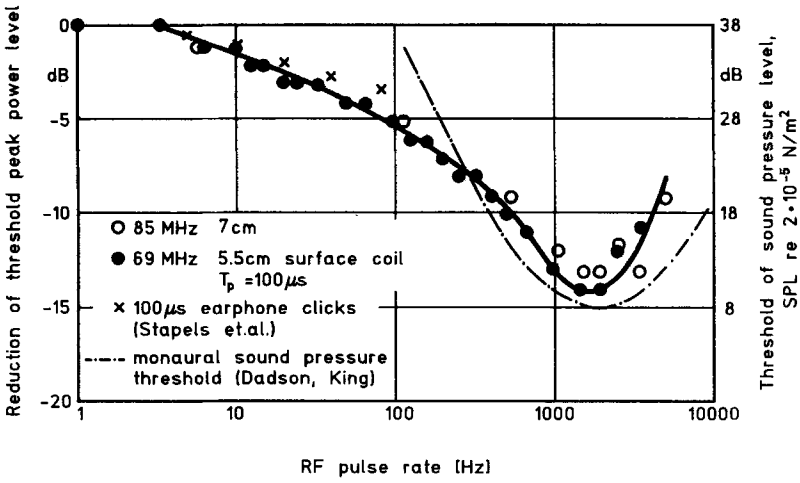

FIG. 6. Reduction of the RF auditory threshold as a function of the RF pulse presentation rate for two MR surface coils positioned flush with the ear. RF pulse trains of 300 ms duration were applied with a repetition time of 1.2 s (3 s for pulse rates above 2500 Hz). For comparison, absolute values of the threshold sound pressure level (SPL) as reported for the external acoustic stimuli of 100 μs earphone clicks and monaurally applied pure tones are shown with the decibel scales fitted at the 5-Hz earphone click threshold. There is an incremental factor of 2 between the decibel scales since the sound pressure amplitude is proportional to the RF peak power per pulse for constant pulse length.

hand ordinate of Fig. 6. The same scale was used to present the monaural pure tone thresholds.

The increments in the decibel scales for the RF power level (RFPL) and for SPL in Fig. 6 differ by a factor of 2, which arises for sound pressure generated by RF energy via thermoelastic expansion. The peak of the sound pressure amplitude (SPA) produced by the absorbed RF energy of a short pulse is (*13*)

$$\text{SPA} \propto T_p \cdot P_a. \qquad [2]$$

The standard decibel definitions for RF power and acoustic sound pressure levels are

$$\text{RFPL [dB]} = 10 \log_{10} P_a / P_{ref}, \qquad [3]$$

$$\text{SPL [dB]} = 20 \log_{10} \text{SPA}/\text{SPA}_{ref}, \qquad [4]$$

where P_{ref} and SPA_{ref} are reference values of RF power and sound pressure, respectively. Inserting [2] in [4] and comparing the result with [3] yields the factor of 2 in

$$\text{SPL [dB]} = 2\ \text{RFPL [dB]} + \text{offset [dB]}. \qquad [5]$$

The offset in [5] depends on the reference values used. In Fig. 6 the offset takes the value of 38 dB as a result of the curve fitting at 5 Hz with SPL threshold results for 100 μs earphone clicks. According to [5], a 1-dB rise in RF power leads to a 2-dB increase in SPL. This explains why the thresholds for the psychophysical RF auditory

phenomenon are observable within such narrow boundaries of only 1-dB RF power variation.

The features of the auditory thresholds shown in Fig. 6 for RF-evoked sound, which may be regarded as effective internal acoustic stimulus, and for the external acoustic sound stimuli are quite similar for clicks at pulse rates up to 20 Hz as well as for pure tones in the interval from 300 to about 3000 Hz. This coheres with the specifics of perception of the RF-evoked sound at different pulse rates. The 300-ms RF pulse trains were heard as distinct clicks at rates up to about 20 Hz; a buzzing or hissing sound occurred with rising pitch in the 30- to 300-Hz range; at rates above 500 Hz the sound appeared as a more or less pure tone with audio frequency corresponding to the pulse rate. The minimum threshold levels at 2000 Hz of RF-evoked sound and of pure tones agree quite well on the SPL scale obtained from curve fitting with hearing thresholds of earphone clicks. The rapid rise of the RF auditory thresholds at pulse rates above 2500 Hz probably results to a large extent from the used RF pulse length of 100 μs in relation to the period of the fundamental audio frequency. With the rising RF pulse density at high pulse rates, the thermal inertia of tissue leads to changes in the thermoelastic response waveform which in turn modify the spectral intensities of the launched pressure waves.

The observed changes in threshold and perception of RF-evoked sound for different pulse lengths or presentation rates reflect various interactions along the path from initial RF energy absorption to final sound detection in the cochlea. Involved are the complex dielectric and acoustic properties of different kinds of tissue such as brain or bone, as well as the complicated boundary conditions given by the human head, and finally, the behavioral or psychophysical properties of the analyzing and signal processing auditory system.

DISCUSSION

Comparison of RF Auditory Thresholds for MR Coils and Near Field Antenna Exposures

RF auditory thresholds from antenna measurements reported in the literature (*1–4*) for humans and cats as a function of the RF pulse length are compared in Fig. 7 with the range of thresholds observed in this study. The peak power absorption scale for threshold results obtained with MR coils was adjusted to the peak power density scale of the literature data for near field antenna measurements by assuming an effective cross section of absorption of 400 cm^2 for the human head. After applying a correction for the dependence of the RF thresholds on the pulse rate (see Fig. 6), most of the literature data reported for frequencies betwen 425 and 3000 MHz fall into the range of thresholds observed with MR coils for 2.4 to 170 MHz. Two data points from the 3000-MHz data set (*4*) are still 3- or 6-dB below the inferred minimum of the energy density threshold of 9 $\mu J/cm^2$. However, it is noticeable that most of the 3000-MHz data for humans and cats are systematically about 4 dB below another, more comprehensive data set reported for 2450 MHz (*3*). Moreover, there is a general problem in measuring the effective power density for objects in the near field zone of antennas. The near field or Fresnel zone is defined for antennas with aperture D and the free

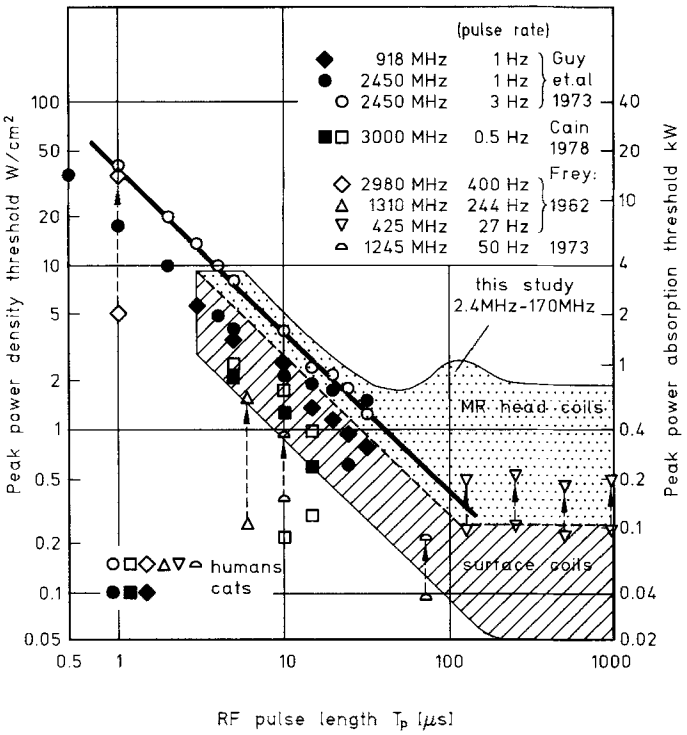

FIG. 7. Comparison of RF auditory thresholds reported in the literature for near field exposure by microwave antennas with the range of thresholds from MR coils observed in this study versus the RF pulse length. The peak power absorption scale was adjusted to the peak power density scale by assuming an effective head area of absorption of 400 cm^2. The dashed arrows denote pulse rate effects on the threshold data reported for high pulse rates, thereby an apt comparison between the data sets is purported.

space wavelength λ as: $R \leq 2D^2/\lambda$. For exposure with an approximately planar wave from a moderately directional antenna having $D \approx 2.5\lambda$, it is required to place the object at a distance of $R > 13\ \lambda$ from the antenna aperture which results in a considerably lowered density of available RF power. The reported thresholds for 3000 MHz were obtained with the back of the head facing the antenna at a distance of 45 cm (4.5 λ) from the 23 × 26-cm aperture plane of a horn antenna. At this distance the human head with a permittivity of $\epsilon_r \approx 50$ may well act as a RF power collecting lense. Thus, the effective cross section of absorption would be considerably larger than the geometrical cross section of the head, which leads to an increase of the actual power density at the head surface. The reported RF power density thresholds refer to probe measurements of the power density provided by the antennas in the absence of the head and were taken at places where the center of the head (*1, 2*), or the back of the head (*4*) would be located during RF irradiation for auditory threshold measurements. Taking these uncertainties, the particulars of the different experimental boundary conditions, and the randomness of the groups of volunteers into account, there is

a remarkable conformity in the behavioral threshold levels of the RF auditory phenomenon exhibited over more than three decades of radio frequencies from 2.4 to 3000 MHz. Remarkable also is that electrophysiological measurements with small animals like cats (*3, 4*) yielded RF peak power density thresholds quite similar to results from RF hearing tests with humans.

Mechanisms of RF to Acoustic Energy Conversion

Explanations of where and how RF energy converts to audible sound can be postulated from the RF auditory thresholds measured as a function of the RF pulse length with different MR coils. Depending on the particulars of RF power deposition in the head, either the outer layer of the brain or the porous bony structures of the temporal and mastoid regions at one or both sides of the head seem to be involved mainly as excitation centers of sound waves with different characteristic frequencies. The thermoelastic expansion during absorption of the pulsed RF power launches pressure transients in one or both of these regions and finally excites pressure waves at one or several of the acoustic eigenfrequencies in the head. If the RF pulse length is short compared to the period $1/f_s$ of the involved sound frequency, a constant threshold of RF pulse energy, $P_{thr} \cdot T_p$, is required to elicit the RF auditory effect (see Figs. 2–5). For long RF pulses, however, only the initially deposited part $P_{thr}/2f_s$ of the pulse energy contributes to the RF–acoustic conversion. This leads to the property of $P_{thr}(T_p)$ = const. observed in Figs. 2–5. A destructive interference effect occurs if $T_p \approx n/f_s$ with resultant relative maxima for $n = 1$ (sometimes also $n = 2$) observable in the oscillatory course of $P_{thr}(T_p)$. Relative minima of $P_{thr}(T_p)$ are given for pulse lengths equal to odd multiples of the half-period of the sound frequency, $T_p \approx (n - 1/2)/f_s$.

The common positions of the threshold minima at 300 μs and of the secondary maxima at 600 μs observed in Fig. 3 for head coils with an anterior–posterior or a caudal–cranial (2.4 MHz)-oriented B_1 field and in Fig. 5 for surface coils positioned flush with the ear correspond according to the interference model to an involved sound frequency of 1700 Hz. This characteristic frequency also agrees well with the threshold minimum observed for 100 μs pulses at pulse rates between 1500 and 2000 Hz (see Fig. 6). In these considered cases, RF power deposition is more or less confined to the bony structures of the temporal and mastoid region of the skull. In fact, the lowest threshold levels were found with a 7-cm surface coil displaying almost ideally the expected W_{thr} = const. and P_{thr} = const. characteristics in Fig. 5. Placed next to the ear, surface coils with optimized size and position probably deposit most of the delivered RF energy into the nearby temporal and mastoid bony masses rather than into the pinna and relatively thin layer of skin in between. It is therefore plausible to assume that these bony structures act as an excitation center for a vibrating resonance mode of the skull with resonance frequency f_{sk} = 1700 Hz. With increasing coil diameter or unfavorable position, an increasing part of the RF energy is deposited either in acoustically inactive tissue regions or in adjacent brain tissue. As a result, not only the threshold levels increase (see Fig. 5) but also another additional sound frequency in the 10 to 12 kHz range appears to be involved in the RF acoustic conversion

process. This holds quite generally for exposure with MR head coils where RF power deposition is confined more or less to the brain. The deviations of $P_{thr}(T_p)$ from the respective linear curves for W_{thr} = const. in the range 30 μs < T_p < 200 μs, (see Figs. 2–5), display the expected features of interference between RF pulse length and sound frequency period at sound frequencies between 10 and 12 kHz.

Particularly well-pronounced interference effects for f_s = 10 kHz are found from the oscillatory course of $P_{thr}(T_p)$ shown in Fig. 2 for a head coil with laterally oriented B_1 field. Here, the major loops of the induced electrical field or eddy currents lie in sagittal planes with pathways parallel to the brain–skull interface. Little RF power is deposited in regions near the axis of the eddy current loops which passes through the mastoid and temporal bone region. However, with the electric field vector parallel to the brain (br)–skull (sk) interface, the ratio of the absorbed power per unit volume is given by the conductivity ratio (*15*)

$$p_{br}/p_{sk} = \sigma_{br}/\sigma_{sk}. \qquad [6]$$

Since $\sigma_{br} \approx 10\sigma_{sk}$ (*14*), the power deposition from eddy current loops passing along the brain–skull interface takes place mainly in the outer layer of the brain reaching from the back via the top to the front of the head. Likewise a considerable part of the RF power is deposited in acoustically inactive regions of the head outside and below the skull decreasing the efficiency of RF–acoustic conversion with resultant higher RF threshold levels.

If a substantial part of the impinging RF energy is absorbed in the brain, conversion to audible sound involves predominantly the fundamental vibrational resonance mode of the brain. Compared to predominant bone excitation this leads to quite different features in the threshold dependence of RF pulse length as can be seen from Figs. 2 and 4. For the brain surface confined by the rigid skull and assuming a spherical shape, the fundamental acoustic resonance frequency of the brain is given by (*6*)

$$f_{br} = 0.71v/a, \qquad [7]$$

where v = 1460 m/s is the velocity of sound in brain matter and $a \approx 9 \pm 1$ cm is the effective radius of the brain–skull structure. The characteristic sound frequencies of 10 to 12 kHz inferred from the $P_{thr}(T_p)$ oscillations in the range 30 μs < T_p < 200 μs agree well with the result from [7], $f_{br} \approx 11.7 \pm 1.3$ kHz. Direct measurements of RF-evoked acoustic pressure wave excitations at the brain mode resonance frequency have been reported (*16*) for small animals exposed to short microwave pulses well above the auditory threshold level. The response from a hydrophone transducer, which was implanted approximately 1.5 cm deep in the brain, clearly showed acoustic brain mode vibrations near 40 kHz for a cat, 60 kHz for rats. All these results are close to the theoretical predictions (*6*) from the thermoelastic conversion model, Eq. [7].

The thresholds shown in Fig. 5 for the 7 cm, 85 MHz surface coil placed next to the ear and in Fig. 2 for a head coil with laterally oriented B_1 field represent examples for an almost exclusive excitation either of the skull model or of the brain mode vibrations, respectively. Only on first sight the conversion to the skull mode apparently exhibits a considerably higher efficiency than the conversion to the brain mode. However, a quantitative comparison based on the lowest pulse energy threshold of 3.6 mJ

for the skull mode requires an apt consideration of the varying amount of RF power deposited for different coil–head configurations in acoustically inactive tissue regions. Moreover, the RF pulse length interference effect leads for $T_p > 1/f_s$ to a constant level of RF power threshold which is proportional to the involved sound frequency, hence,

$$P_{thr}(\text{brain})/P_{thr}(\text{skull}) = f_{br}/f_{sk} \approx 6.$$

This proportionality agrees quite well with the ratio of the respectively assigned thresholds from Figs. 2 and 4 for $T_p > 1000$ μs. Since for both of these cases the values of pulse energy thresholds converge for $T_p < 30$ μs, it is reasonable to assume a similar efficiency of RF acoustic conversion for both vibrational modes. However, the behavioral frequency selective property of the human auditory system very likely enhances preferably the perception of sound from the RF-excited skull mode vibrations since $f_{sk} \approx 1700$ Hz is close to the frequency range with maximum hearing sensitivity between 2 and 4 kHz. This explains to a large extent the dominance of skull mode effects observed in most of the experiments.

Other reasons for the dominance of skull mode effects stem from the specifics of RF power deposition. Almost contrary shares of brain and skull mode contributions are inferred from the thresholds in Figs. 2 and 3 for head coils when the B_1 orientation is changed from lateral to the anterior–posterior (a–p) or caudal–cranial (c–c) directions. Similar effects are seen in the threshold characteristics for a surface coil shown in Fig. 4 for different coil locations on the head. In opposition to the earlier discussed case for laterally applied B_1 field, major eddy current loops also pass through the temporal and mastoid bone regions when the B_1 fields of head coils are applied in the a–p or c–c directions. Wherever in these regions the resultant electric field vector is perpendicular to the interface between skull bones and brain or other soft tissues, the ratio of RF power absorption per unit volume is given by (*15*)

$$\frac{p_{sk}}{p_{br}} = \frac{\sigma_{sk}}{\sigma_{br}} \left(\frac{\epsilon_{br}}{\epsilon_{sk}} \right) \frac{1 + \tan^2\delta_{br}}{1 + \tan^2\delta_{sk}}, \qquad [8]$$

where the loss tangent is equal to the ratio of the imaginary and real components of the complex permittivity, $\tan \delta = \epsilon''/\epsilon' = \sigma/\omega\epsilon_0\epsilon_r$, with free space permittivity ϵ_0. Calculations for frequencies up to 300 MHz with reported values of σ and ϵ for the involved tissues (*14*) give an enhancement factor of $p_{sk}/p_{br} \approx 10$ for the power absorption per unit volume. Although the volume of skull bones considered in the perpendicular electric field condition is much smaller than the volume of the outer layer of brain tissue participating in the RF absorption and acoustic conversion process, the combined effect of enhanced local power absorption and enhanced behavioral perception leads to a prevailing share of the skull mode vibrations in the RF auditory effect for a–p- or c–c-oriented homogeneous B_1 fields from MR head coils (see Figs. 2 and 3).

Localized power deposition with the inhomogeneous B_1 field of surface coils obviously excites additional head resonance modes when the coils is placed at locations other than close to the ear. From the pulse length interference concept applied to the thresholds in Fig. 4 for the coil position at the top of the head, resonance modes are

tentatively assigned as brain modes at 20 and 10 kHz, and skull modes at 3.3 kHz and possibly 1 kHz. The individual shares of these different modes are perceptively filtered by the frequency selective auditory system. Simultaneous excitation and participation of various modes in the RF hearing phenomenon may lead to the smoothed $P_{thr}(T_p)$ characteristic measured for the coil position at the back of the head. The nodes and antinodes of the vibrational skull modes are expected at generally fixed, mode specific, positions on the head since shape and thickness of the skull are far from being isotropic. The excitation of a specific skull mode via thermoelastic expansion from localized RF power deposition with surface coils is then possible only at certain locations on the head. This could be the cause of the excitation of entirely different skull modes when the coil location is changed from the ear to the top of the head, as inferred before from the features of the thresholds shown in Fig. 4.

Another noteworthy sound propagation effect is deducible from the earlier mentioned observation that the curves of the W_{thr} = const. and P_{thr} = const. characteristics intersect at distinct values of T_p, which occur at $T_p \approx 120$ μs for bilateral excitation with MR head coils and at $T_p \approx 200$ μs for single-sided excitation with surface coils on the ear. These values correspond fairly well with the propagation time of sound in the head, $t_s = b/v \approx 100$ μs, from one side to the other side of a head with breadth $b \approx 15$ cm and sound velocity $v = 1460$ m/s. For bilateral RF excitation, the pressure transients launched simultaneously from both sides of the head interact with thermoelastic pressure generation at the opposite sides if $T_p > 100$ μs. A pressure transient launched by single-sided RF excitation is reflected at the opposite head side and interacts with further RF acoustic conversion at the origin if $T_p > 200$ μs. These propagation effects determine the finally constant values of the lowest threshold power levels $P_{thr}(\min)$ in Figs. 2–5 which for RF pulse lengths above t_s (head coils) or $2t_s$ (surface coils) are given by $P_{thr}(\min) = W_{thr}(\min)/t_s$ or $W_{thr}(\min)/2t_s$, respectively. The presence of superimposed interference effects between the RF pulse length and the period of sound frequency for the excited skull resonance mode indicates an opposite sign (or phase) for the stimulating pressure transients associated with the leading or trailing edges of the RF pulses.

Conditions for Hearing MR Excitation Pulses

The thresholds of 2.4 and 3.6 mJ obtained for different volunteers with a 7-cm surface coil (see Table 1, Fig. 5) represent the lowest threshold energies thus far observed with MR surface coils. About five times as high are the threshold energies of 16 ± 4 mJ (Fig. 3) measured with MR head coils, which indicates that more than 80% of RF power is deposited in acoustically inactive tissue regions. For pulse lengths $T_p > 100$ μs, the range of auditory thresholds of typically 175 ± 75 W as observed with MR head coils concurs in many cases with the required levels of RF peak power for MR excitation pulses used in MR imaging or spectroscopy investigations of the human head. The dependence of RF power deposition in the head on MR parameters such as flip angle α, pulse width T_p, and MR observe frequency ($\omega = \gamma B_0$) or the static main field strength B_0 is given by

$$\frac{P(\alpha, T_p, B_0)}{[W]} \approx 25 \cdot 10^{-6}\left(\frac{\alpha}{\pi T_p}\right)^2\left(\frac{B_0}{[T]}\right)^{2.2}, \qquad [9]$$

using experimental results reported elsewhere (*17*) for head coils with linearly polarized B_1 fields and for a rectangular RF pulse shape. The relationship to B_0 was chosen in Eq. [9] since RF power deposition for a given (α, T_p) pulse is nearly the same for all MR sensitive nuclei with different resonance frequencies at a given value of B_0 (*17*). The conditions for an auditory perception of MR excitation pulses ($T_p > 100$ μs) are found by equating [9] with the above mentioned typical range of auditory threshold power levels:

$$\frac{T_p}{\text{ms}} \leq (0.4 \pm 0.1)\frac{\alpha}{\pi}\left(\frac{B_0}{[T]}\right)^{1.1}. \qquad [10]$$

For quadrature head coils with a circularly polarized B_1 field and a MR excitation power theoretically reduced by 3 dB, the numeric factor in [10] is 0.3 ± 0.07 when taking anisotropic RF absorption effects (*17*) into account. If not masked by the usually dominating noise from simultaneously switched gradients or by auditory fatigue, patients might hear π pulses in MR sequences during head studies performed with 0.5-T systems when hard RF pulses, $T_p \leq 0.2$ ms, are used. For a 2-T system, π pulses of 1 ms duration already meet the condition [10] for RF hearing.

RF transmitter power levels up to 15 kW are not uncommon in high-field MR systems. At this power level, if applied to the human head with a head coil, the perceived RF-evoked sound would according to Eq. [5] be about 40 dB above the pressure level at the RF hearing threshold (about 150 W, Fig. 3). Based on the equivalent pressure amplitude of 38 dB SPL at the RF hearing threshold (Fig. 6), the perception level of the internal sound stimuli evoked in the head by 15 kW RF pulses corresponds to 78 dB SPL. This level appears still harmless in comparison with accepted levels of 93 ± 10 dB(C) for externally impressed noise from switched gradients (*18*). However, the actual sound pressure level in the head is very likely higher than the inferred perceptional equivalent of 78 dB SPL since bone conduction is involved in the RF hearing process. The differences in thresholds for air conduction and bone conduction is about 50 ± 5 dB for externally applied sound stimuli (*19*). Simply adding these values for internal and external stimuli probably gives an overestimate for the actual peak pressure of 128 ± 5 dB SPL, which would be close to the hazardous range of pain threshold at 140 dB SPL (*20*) for the human auditory system. Somewhat lower values of actual sound pressure may be inferred from different arguments. Body-conducted sound arriving via final bone conduction at the cochlea is not transformed by the ear drum–ossicle bone chain–oval window route with approximately 26 dB gain in sound pressure (*20*). For this condition the actual sound pressure level in the head would be 26 dB above the perceptional (15 kW RF-evoked) value of 78 dB SPL, i.e., 104 dB SPL. A similar SPL value is derived from experimental data reported for thermally generated pressure transients in water at 25°C by pulsed microwaves (*13*) where 5.3 W/cm^2 pulses produced peak pressure transients with 100 dB SPL. At 37°C the corresponding value is 103 dB SPL due to the temperature dependence of the thermal expansion coefficient of water (*13*). For 15 kW and an effective head area of

absorption of 400 cm^2, the sound pressure is 120 dB SPL. This value reduces to 106 dB SPL when accounting for 80% RF power deposition in acoustically inactive tissue regions.

Health Aspects

The question of whether possible health risks are associated with the RF auditory phenomenon, especially with regard to direct interaction effects of RF irradiation on the central nervous system, has been raised before (*21, 22*). Obvious implications on health issues other than tissue heating by RF exposure at average power levels exceeding the recommended limit of 5 W/kg have not been found as yet. A hazardous level of the RF-evoked pressure transients in the head is avoided if the peak power of RF pulses ($T_p > 100$ μs) applied to MR head coils is limited to an upper level of about 30 kW (6 kW for surface coils). This value has been based on the discomfort threshold at 110 dB SPL (*20*) for external sound stimuli, and on the internal peak pressure transient of 104 dB SPL as deduced earlier for 15 kW pulses. The equivalence assumed for the external and internal acoustic stimuli levels is questionable in this context. However, the hazardous thresholds of external sound stimuli for pain at 140 dB SPL and for damage to the auditory system at 150 to 160 dB SPL (*20*) are still several orders of magnitude above the internal level near 110 dB SPL that is likely to be evoked by 30 kW RF pulses. A lowered level of the tolerable pulse peak power could result from considerations of detrimental physiological reactions, if any, to nonthermal RF effects. The role of proposed nonthermal effects of RF exposure on biological systems and human physiology is a controversial subject due to the lack of reliable and reproducible experimental results (*22–25*). In attempting to relate effects from RF exposure to nonthermal mechanisms, it is extremely difficult to rule out other environmental factors or to exclude the possibility of primary local heating as the cause of a secondary biophysical mechanisms for the observed effects (*23, 25*).

In the search for potential neurophysiological interactions caused by RF electromagnetic fields or energy, the auditory sensory system excels as guidance tool for experimentation due to its extremely high sensitivity to physical stimuli. Compared to the ultimate threshold sensitivity of the retinal rod, which is given by the single photon energy of $4 \cdot 10^{-19}$ J, the threshold response of a single cochlear hair cell corresponds to about 10^{-20} J (*26*). However, the combined effects of approximately 50 photons are required to elicit visual perception, and similarly, about 100 hair cells on the basilar membrane must be cooperatively excited by sound energy to elicit an auditory response (*26*). The absence of any other kind of nonauditory neural sensory perception during the RF exposure with widely varied parameters, although not fully conclusive with regard to the conspicuous role of audition sensitivity, provides a strong argument against significant neuro interaction effects at the used RF levels. The possibility of a direct interaction of RF with the auditory nerves or neurons in the higher structures of the auditory perception route appears more and more unlikely in view of the manifold evidence from experiments substantiating the thermoelastic expansion mechanism as a secondary cause associated with the primary RF to thermal energy conversion.

ACKNOWLEDGMENTS

The author thanks Dr. J. Wieland for adapting suitable test sequences, for the execution of threshold measurement series with the author being subject, and for valuable discussions. This work was funded in part by the Federal Republic of Germany, Bundesministerium für Forschung und Technologie (BMFT).

REFERENCES

1. A. H. FREY, *J. Appl. Physiol.* **17,** 689 (1962).
2. A. H. FREY AND R. MESSENGER, JR., *Science* **181,** 356 (1973).
3. A. W. GUY, E. M. TAYLOR, B. ASHLEMAN, AND J. C. LIN, *IEEE Trans. Microwave Theory Tech. Int. Symp. Dig.,* 321 (1973).
4. C. A. CAIN AND W. J. RISSMANN, *IEEE Trans. Biomed. Eng.* **BME-25,** 288 (1978).
5. D. E. BORTH AND C. A. CAIN, *IEEE Trans. Microwave Theory Tech.* **MTT-25,** 944 (1977).
6. J. A. LIN, *IEEE Trans. Micorwave Theory Tech.* **MTT-25,** 605, 938 (1977).
7. P. RÖSCHMANN AND J. WIELAND, *in* "Book of Abstracts, Eighth Annual Meeting, Society of Magnetic Resonance in Medicine, Amsterdam, 1989," p. 292.
8. H. BOMSDORF, T. HELZEL, D. KUNZ, P. RÖSCHMANN, O. TSCHENDEL, AND J. WIELAND, *NMR Biomed.* **1,** 151 (1988).
9. C. LEUSSLER AND W. VOLLMANN, *in* "Book of Abstracts, Eighth Annual Meeting, Society of Magnetic Resonance in Medicine, 1989," p. 938.
10. J. C. SLATER, "Microwave Electronics," pp. 98–102, Van Norstrand, Princeton, 1950.
11. D. R. STAPELLS, T. W. PICTON, AND A. D. SMITH, *J. Acoust. Soc. Am.* **72,** 74 (1982).
12. R. S. DADSON AND J. H. KING, *J. Laryngol. Otol.* **46,** 336 (1952).
13. K. R. FOSTER AND E. D. FINCH, *Science* **185,** 256 (1974).
14. C. C. JOHNSON AND A. W. GUY, *Proc. IEEE* **60,** 692 (1972).
15. W. T. JOINES, *IEEE Trans. Biomed. Eng.* **BME-31,** 17, (1984).
16. R. G. OLSEN AND J. C. LIN, *IEEE Trans. Biomed. Eng.* **BME-30,** 289 (1983).
17. P. RÖSCHMANN, *Med. Phys.* **14,** 933 (1987).
18. R. HURWITZ, S. R. LANE, R. A. BELL, AND M. N. BRANT-ZAWADZKI, *Radiology* **173,** 545 (1989).
19. J. SCHRÖTER AND H. ELS, *Acustica* **50,** 250 (1982).
20. L. L. BERANEK, "Acoustics," pp. 388–406, McGraw–Hill, New York, 1954.
21. J. C. LIN, *Proc. IEEE* **68,** 67 (1980).
22. A. H. FREY, *IEEE Trans. Microwave Theory Tech.* **MTT-19,** 153 (1971).
23. S. M. MICHAELSON, *Proc. IEEE* **68,** 40 (1980).
24. O. P. GANDHI, *IEEE Trans. Microwave Theory Tech.* **MTT-30,** 1831 (1982).
25. T. F. BUDINGER, *J. Comp. Asst. Tomogr.* **5,** 860 (1981).
26. A. H. GITTER AND R. KLINKE, *Naturwissenschaften* **76,** 160 (1989).